0026-895X/10/7705-759–772$20.00
MOLECULAR PHARMACOLOGY
Copyright © 2010 The American Society for Pharmacology and Experimental Therapeutics
Mol Pharmacol 77:759–772, 2010

Vol. 77, No. 5
61432/3580566
Printed in U.S.A.

H2 Relaxin Is a Biased Ligand Relative to H3 Relaxin at the Relaxin Family Peptide Receptor 3 (RXFP3)[S]

Emma T. van der Westhuizen, Arthur Christopoulos, Patrick M. Sexton, John D. Wade, and Roger J. Summers

Drug Discovery Biology, Monash Institute of Pharmaceutical Sciences, Parkville, Victoria, Australia (E.T.v.d.W., A.C., P.M.S., R.J.S.); Department of Pharmacology, Monash University, Clayton, Victoria, Australia (E.T.v.d.W., A.C., P.M.S., R.J.S.); and Howard Florey Institute, University of Melbourne, Parkville, Victoria, Australia (J.D.W.)

Received October 1, 2009; accepted February 4, 2010

ABSTRACT

Relaxin family peptide 3 receptors (RXFP3) are activated by H3-relaxin to inhibit forskolin-stimulated cAMP accumulation and stimulate extracellular signal-regulated kinase (ERK) 1/2 phosphorylation. In this study, we sought to identify novel signaling pathways coupled to RXFP3 and to investigate whether other members of the relaxin peptide family activated these pathways. Two patterns of signaling were observed in RXFP3-expressing Chinese hamster ovary (CHO)-K1 and human embryonic kidney (HEK)-293 cells (CHO-RXFP3 and HEK-RXFP3) and murine septal neuron SN56 cell lines: 1) strong inhibition of forskolin-stimulated cAMP accumulation, ERK1/2 activation and nuclear factor (NF)-κB reporter gene activation in cells stimulated with H3 relaxin, with weaker activity observed for H2 relaxin, porcine relaxin, or insulin-like peptide (INSL) 3 and 2) strong stimulation of activator protein (AP)-1 reporter genes by H2 relaxin, with weaker activation observed with H3 or porcine relaxin. Two distinct ligand binding sites were identified on RXFP3-expressing cells using two different radioligands. ^{125}I-INSL5 A-chain/relaxin-3 B-chain chimera bound with high affinity to the RXFP3-expressing cells with competition by H3 relaxin or a H3 relaxin B-chain dimeric peptide, consistent with previous reports. Binding studies with ^{125}I-H2 relaxin revealed a distinct binding site with potent competition observed with H2 relaxin, H3 relaxin, or INSL3 and weaker competition with porcine relaxin. Thus H3 relaxin potently activates all signaling pathways coupled to RXFP3, whereas H2 relaxin is an AP-1-biased ligand relative to H3 relaxin.

The neuropeptide relaxin-3 is the most recently identified member of the relaxin family of peptides and is expressed in the nucleus incertus, acting at relaxin-3 receptors (RXFP3) expressed at distal sites (Bathgate et al., 2002). Relaxin-3 expression is up-regulated in response to physical stress in rats by a corticorelin-dependent mechanism (Tanaka et al., 2005), suggesting a role in mediating central stress responses. Relaxin-3 injection into the paraventricular nucleus of the hypothalamus or the fourth ventricle increased food intake in rats (McGowan et al., 2007), also indicating a role in appetite control acting via its cognate receptor, RXFP3. Development of ligands that target RXFP3 would potentially provide drugs for the treatment of obesity and anxiety disorders.

This work was supported by the National Health and Medical Research Council (NHMRC) of Australia [Project Grants 436713 (to R.J.S.), 454375 (to J.D.W.), Program Grant 519461 (to R.J.S., A.C., P.M.S.)]; an NHMRC Dora Lush (Biomedical) Postgraduate Scholarship (to E.T.v.d.W.); an NHMRC Principal Research Fellowship (to P.M.S.); and NHMRC Senior Research Fellowship (to A.C.).

Portions of this work have appeared previously in the following forms: van der Westhuizen E.T., "Molecular characterization of human and mouse relaxin-3 receptors (RXFP3) in recombinant and endogenously expressing cell lines," Ph.D. Thesis, Monash University, Australia; Experimental Biology 2007, Washington DC, 28 Apr–2 May 2007; Experimental Biology 2008, San Diego, CA, 5–9 April 2008; 5th International Conference on Relaxin and Related Peptides, Maui, HI, 18–23 May 2008; Australian Health and Medical Research Congress 2008, Brisbane, Australia, 16–21 Nov 2008; and the British Pharmacological Society's 3rd Focused Meeting on Cell Signalling, Leicester, UK, 20–21 April 2009.

Article, publication date, and citation information can be found at http://molpharm.aspetjournals.org.

doi:10.1124/mol.109.061432.

[S] The online version of this article (available at http://molpharm.aspetjournals.org) contains supplemental material.

ABBREVIATIONS: AP-1, activator protein 1; BSA, bovine serum albumin; CHO-RXFP3, Chinese hamster ovary-K1 cells expressing RXFP3; DMEM, Dulbecco's modified Eagle's medium; ERK, extracellular signal-regulated kinase; FBS, fetal bovine serum; GFP, green fluorescent protein; GPCR, G protein-coupled receptor; GTPγS, guanosine 5′-*O*-(3-thio)triphosphate; H2 relaxin, human gene 2 relaxin; H3 relaxin, human gene 3 relaxin; HEK-RXFP3, human embryonic kidney 293 cells expressing RXFP3; INSL, insulin-like peptide; JNK, c-Jun N-terminal kinase; MAPK, mitogen-activated protein kinase; MEK, mitogen-activated protein kinase kinase; NF-κB, nuclear factor κB; PD98059, 2′-amino-3′-methoxyflavone; PI3K, phosphatidylinositol 3-kinase; PKC, protein kinase C; PTX, pertussis toxin; RT-PCR, reverse transcription-polymerase chain reaction; RWJ67657, 4-[4-(4-fluorophenyl)-1-(3-phenylpropyl)-5-(4-pyridinyl)-1*H*-imidazol-2-yl]-3-butyn-1-ol; RXFP, relaxin family peptide receptor; SB203580, 4-(4-fluorophenyl)-2-(4-methylsulfinyl phenyl)-5-(4-pyridyl)1*H*-imidazole; SEAP, secreted alkaline protease; SN56, mouse septal neuron-derived cell line; SP600125, anthra[1,9-*cd*]pyrazol-6(2*H*)-one; TFA, trifluoroacetic acid.

The term ligand-directed signaling, among other synonyms, was coined to describe the distinct efficacy profiles observed for different signaling pathways by individual ligands. Typically, activated GPCRs (bound to their cognate ligand) fully activate all the signaling pathways coupled to the receptor. However, several studies have identified that many compounds classified as antagonists can activate their own spectrum of signaling pathways. Thus propranolol (traditionally classified as a β-adrenoceptor antagonist) acts at the β_1-adrenoceptor as an inverse agonist for cAMP signaling but as a partial agonist for ERK1/2 signaling (Galandrin and Bouvier, 2006), suggesting that the signaling assay selected as a measure of the response can bias the classification of a ligand. However, many GPCRs, including the α- and β_3-adrenergic, 5-hydroxytryptamine, dopamine, opioid, adenosine, calcitonin, and muscarinic acetylcholine receptors, are activated by multiple ligands, each with distinct affinity, efficacy, and potency profiles (Kenakin, 2003; for review, see Baker and Hill, 2007).

To activate different signaling pathways, GPCRs may couple to multiple Gα-subunits (e.g., Gα_s and G$\alpha_{i/o}$), but signaling may also occur downstream of G$\beta\gamma$-subunits or after β-arrestin recruitment and may not even involve G proteins. In addition, movement of GPCRs into or out of membrane rafts after ligand binding can switch the Gα-coupling and initiate additional signaling events providing another mechanism for GPCR coupling to multiple signal transduction pathways (for review, see Chini and Parenti, 2004).

RXFP3 is known to inhibit forskolin-stimulated cAMP accumulation and activates ERK1/2 in a G$\alpha_{i/o}$-dependent manner (Liu et al., 2003; van der Westhuizen et al., 2007) and thus resembles many other GPCRs that couple to multiple signaling pathways when stimulated by their cognate ligand. RXFP3 was originally characterized by high-affinity binding of H3 relaxin and little or no affinity for other members of the relaxin peptide family (Liu et al., 2003). H3 relaxin potently inhibits forskolin-stimulated cAMP accumulation in RXFP3-expressing cells, consistent with competition binding data (Liu et al., 2003). Furthermore, increases in GTPγS binding are evident only in cells stimulated with H3 relaxin or the B-chain of H3 relaxin (Liu et al., 2003), suggesting that the other members of this peptide family do not strongly activate G protein-dependent signaling pathways.

Despite the close homology between the relaxin family peptides, it was interesting that binding and signaling by other members of this peptide family was not observed at RXFP3. However, recent experience with GPCRs suggests that multiple signaling pathways should be monitored to determine whether a ligand has biased efficacy at a particular receptor. This study examined whether additional signaling pathways were activated by RXFP3 after stimulation with H3 relaxin and determined whether other members of the relaxin peptide family could also activate signaling. CHO-RXFP3, HEK-RXFP3, and murine SN56 septal neuron-derived cells were characterized using binding and signaling assays. We identified, using reporter genes, two novel signaling pathways activated downstream of RXFP3 (the NF-κB signaling pathway and pathways upstream of AP-1 transcription sites) and demonstrated that many of the relaxin family peptides have affinity for RXFP3 and efficacy on AP-1 signaling. RXFP3 also has a binding site that recognizes H2 relaxin with a unique pharmacological profile compared with that described for RXFP1 and RXFP2. Thus we propose a novel site on RXFP3 that can interact with several relaxin peptides and that activation of the receptor by the various peptides results in activation of different signaling pathways.

Materials and Methods

Materials. Flp-InCHO and Flp-In293 cells, TRIzol, Lipofectamine, OptiMEM, hygromycin B, and Fungizone were from Invitrogen (Carlsbad, CA). SN56 cells were a gift from Dr. R. A. D. Bathgate (Howard Florey Institute, Melbourne, Australia). RQ1 DNase and avian myeloblastosis virus reverse transcriptase were from Promega (Madison, WI). Secreted alkaline phosphatase (SEAP) reporter gene constructs were from Clontech (Mountain View, CA). Dulbecco's modified Eagle's medium (DMEM), DMEM/Ham's F12 powder media and penicillin/streptomycin were from ThermoTRACE (Melbourne, Australia). Fetal bovine serum (FBS) was from JRH Biosciences (Lenexa, KS). The cAMP AlphaScreen assay kit, Protein A beads, and white 96-well and 384-well Optiplates were from PerkinElmer Life and Analytical Sciences (Wellesley, MA). Surefire phospho-ERK kit was from TGR Biosciences (Adelaide, Australia). Forskolin was from Sigma Aldrich (St. Louis, MO). Tissue culture flasks and plates were from Greiner Bio-One (Monroe, NC). Human insulin-like peptide (INSL) 3, human gene 3 relaxin (H3 relaxin) (Bathgate et al., 2006), and INSL5 A-chain/relaxin-3 B-chain chimera (Sutton et al., 2004) were synthesized at the Howard Florey Institute (Victoria, Australia). Human gene 2 relaxin (H2 relaxin) was supplied by Corthera Inc. (San Mateo, CA), and porcine relaxin was extracted from ovaries and purified at the Howard Florey Institute (Layden and Tregear, 1996).

Cell Culture. Stable RXFP3-expressing cells, created using Flp-InCHO and Flp-In293 cells expressing human RXFP3 (CHO-RXFP3 and HEK-RXFP3, respectively) (van der Westhuizen et al., 2007) were maintained in 75-cm^2 flasks at 37°C in a humidified atmosphere in DMEM/Ham's F12 medium (CHO-RXFP3) or DMEM (HEK-RXFP3 and SN56). DMEM/Ham's F12 was supplemented with 5% (v/v) FBS, 2 mM L-glutamine, 100U/ml penicillin, 100 μg/ml streptomycin, and 0.5 μg/ml Fungizone. DMEM was supplemented with 10% (v/v) FBS, 4 mM L-glutamine, and antibiotics as above.

Whole-Cell Radioligand Binding Assays. H2 relaxin and INSL5/H3 relaxin chimera were iodinated with Na^{125}I using the chloramine T method (Sexton et al., 1986). The iodinated peptides (specific activity, ~2200 Ci/mmol) were purified by high-performance liquid chromatography. Cells (10^5 cells/well) were plated into 48-well plates and grown for 18 h at 37°C. Binding was performed at room temperature (23 ± 2°C) for 90 min. Competition for ^{125}I-INSL5/relaxin-3 (100 pM) binding was terminated by aspirating the binding buffer and washing the cells twice with ice-cold PBS, then lysing in NaOH (0.5 M) and counting in a Wallac Wizard 1470 automatic gamma-counter (PerkinElmer Life and Analytical Sciences, Waltham, MA). Competition for ^{125}I-H2 relaxin (~1 nM) binding was terminated by placing the plates on ice and rapidly (~0.5 s) washing the cells once with ice-cold PBS, then lysing the cells and counting the samples as described above.

Whole-Cell Internalization Binding Assays. Cells (10^5 cells/well) were plated into 48-well plates and grown for 16 h at 37°C. The cells were transiently transfected with RXFP3-GFP[2] (van der Westhuizen et al., 2009) (100 ng/well) using Lipofectamine according to the manufacturer's instructions. Cells were stimulated in binding buffer (DMEM/Ham's F12 or DMEM, 0.5% BSA, and 25 μM cycloheximide) with H3 relaxin at 37°C for selected time points (5, 10, 15, 30, 45, and 60 min) in a shaking incubator. The plates were placed on ice and washed once with ice-cold PBS then acid-stripped using acid elution buffer (150 mM sodium chloride and 50 mM acetic acid, pH 2.5) for 10 min on ice. The acid was aspirated and the cells were washed three times with ice-cold PBS. The cells were incubated with ^{125}I-INSL5/H3 relaxin chimaera (100 pM) for 4 h on ice. Nonspecific

binding was defined in the presence of H3 relaxin (0.1 μM) at each time point. The cells were washed, solubilized, and counted as described for whole-cell binding assays.

ERK Phosphorylation Assay. Cells (5×10^4 cells/well) were plated into 96-well plates and grown for 27 h in complete DMEM or DMEM/Ham's F-12 medium and then serum-starved for 18 h before experimentation and assayed for phospho-ERK1/2 (Surefire ERK kit; PerkinElmer Life and Analytical Sciences) using a novel non–Western blot-based proprietary technique that relies on the energy transfer-based AlphaScreen concept (Osmond et al., 2005) as described previously (van der Westhuizen et al., 2007). Cells were treated for 2 to 30 min (time course assays) or 5 min (concentration-response curves) with relaxin family peptides at 37°C. As a positive control, cells were stimulated with 10% FBS, up to 30 min for time-course assays or 5 min for concentration-response assays). Cell lysates were prepared and processed according to the manufacturer's protocol. In brief, a 5-μl sample of processed cell lysate was transferred to a white 384-well Optiplate, and 6 μl of a 1:1 mix of Protein A AlphaScreen donor and acceptor beads was added to each well. Plates were incubated for 2 h at 22°C in the dark. Samples were read on a Fusion-Alpha microplate reader (PerkinElmer Life and Analytical Sciences) with excitation at 680 nm and emission at 520 to 620 nm.

Inhibition of Forskolin-Stimulated cAMP Accumulation Assay. Cells were plated and serum-starved as described for the ERK1/2 assay described above. The cAMP AlphaScreen assay kit was used to measure the amount of cAMP generated by the cells upon stimulation with forskolin and its inhibition by relaxin family peptides as described previously (van der Westhuizen et al., 2007). In brief, DMEM was removed from the wells and replaced with stimulation buffer [137 mM NaCl, 5.1 mM KCl, 0.77 mM $MgSO_4 \cdot 7H_2O$, 1.23 mM $CaCl_2 \cdot 2H_2O$, 0.32 mM $Na_2HPO_4 \cdot 2H_2O$, 0.42 mM KH_2PO_4, 5.27 mM D-glucose, 0.5 mM 3-isobutyl-1-methylxanthine, 5 mM HEPES, and 0.1% (w/v) BSA, pH 7.4]. Cells were stimulated for 5 min with relaxin family peptides (1 pM–1 μM) and then for 3 min with forskolin (30 μM) (CHO-RXFP3 and HEK-RXFP3) or 20 min (SN56) in a 37°C shaking incubator. Cells were lysed in lysis buffer [0.3% (v/v) Tween 20, 5 mM HEPES, and 0.1% (w/v) BSA, pH 7.4] at −70°C for 1 h. Cell lysates were thawed on ice, mixed thoroughly, and a 5-μl sample was transferred to a white 384-well Optiplate. Acceptor beads diluted in detection buffer [5.2 mM NaCl, 2 mM KCl, 0.31 mM $MgSO_4 \cdot 7H_2O$, 0.5 mM $CaCl_2 \cdot 2H_2O$, 0.13 mM $Na_2HPO_4 \cdot 2H_2O$, 0.17 mM KH_2PO_4, 2.1 mM D-glucose, 3 mM HEPES, 1.8% (v/v) Tween 20, and 0.1% (w/v) BSA, pH 7.4] were added to each well under ambient light and incubated at 22°C in the dark for 30 min. Donor beads and biotinylated cAMP were also diluted in detection buffer and incubated separately at 22°C in the dark for 30 min. Donor bead/biotinylated cAMP mix was added and incubated for 16 h at 22°C in the dark. Plates were read on a Fusion-Alpha microplate plate reader (PerkinElmer Life and Analytical Sciences) with excitation at 680 nm and emission at 520 to 620 nm.

RNA Extraction and Reverse Transcription-Polymerase Chain Reaction to Detect RXFP Expression. RNA was isolated from CHO-K1, HEK293, CHO-RXFP3, HEK-RXFP3, CHO-RXFP4, HEK-RXFP4, SN56, HEK-RXFP1, and HEK-RXFP2 cells using TRIzol according to the manufacturers' protocol. The RNA was treated with RQ1 DNase, and the RNA (5 μg) was reverse transcribed using avian myeloblastosis virus reverse transcriptase and oligo(dT_{15}) primers for 2 h at 42°C. PCR was performed by 20 to 30 cycles of 94°C for 30 s, 45 to 60°C for 30 s (as described below) and 72°C for 2 min. The primers used crossed several species. Human/mouse/rat RXFP1 and RXFP2 were amplified using 5′-GCCTAGAAATCAAATTGGTTTTGTTCCAGAG-3′(forward) and 5′-ACAAAGGATTTTGATGGACATAGCGTGAG-3′ (reverse) as primers for 25 cycles, annealing at 60°C. Human/mouse/rat RXFP3 was amplified using 5′-GGCAAGGCCATGTGTAAGATC-3′ (forward) and 5′-CGTTGAACTTGATGAGGATGCTCCAG-3′ (reverse) as primers for 30 cycles, annealing at 45°C. Human/mouse RXFP4 was amplified using 5′-CATTGGCTTGCTGGGAAATTTGG-3′ (forward) and 5′-CCAGTACCTGCTGGGGAAACG-3′ (reverse) primers for 30 cycles, annealing at 56°C. β-Actin was amplified as a control using 5′-ATCCTGCGTCTGGACCTGGCTG-3′ (forward) and 5′-CCTGCTTGCTGATCCACATCTGCTG-3′ (reverse) primers for 20 cycles, annealing at 60°C. DNA was electrophoresed for 30 min at 100 V through 1% (w/v) agarose gel, stained with ethidium bromide, and visualized by illumination with UV light.

SEAP-Linked Reporter Gene Assay. Eight *cis*-acting enhancer elements linked to human placental alkaline phosphatase (SEAP; Mercury Pathway Profiling) were used to identify novel signaling pathways downstream of RXFP3 (described in Halls et al., 2007). After reporter gene activation, the levels of SEAP in the culture medium are directly proportional to the changes in intracellular SEAP concentrations. The reporter gene SEAP is modified so it is heat stable, thereby making it possible to eliminate endogenous alkaline phosphatase activity by heat-treating the samples taken from the culture medium. A constitutively expressed β-galactosidase reporter gene was cotransfected with the SEAP reporter gene (1:1) to account for variation in transfection efficiencies between experiments.

Flp-InCHO or Flp-In293 cells (2×10^5 cells/well) were plated into 24-well plates and grown for 24 h at 37°C. Cells were transiently cotransfected with RXFP3 (150 ng/well), SEAP-linked reporter gene (75 ng/well), and β-galactosidase (75 ng/well) in OptiMEM using Lipofectamine according to the manufacturer's protocol. Cells were serum-starved for 18 h, then stimulated with relaxin family peptides (range, 1 pM–0.1 μM), trifluoroacetic acid (TFA) [vehicle control, 0.001% (v/v)] or a positive control (30 μM forskolin for cAMP response element; 1 μM ionomycin for nuclear factor of activated T cells; 42°C, 1 h heat shock for heat shock element; 10% FBS for AP-1, NF-κB, E-box DNA binding element, glucocorticoid response element and serum response element) and samples of the medium were taken at selected time points after stimulation (4 h for AP-1 reporter genes or 8 h for NF-κB reporter genes) and frozen at −20°C. Twenty-five microliters of the thawed samples were transferred to white 96-well Optiplates. SEAP reporter gene samples were incubated at 65°C for 30 min then cooled on ice for 5 min. SEAP assay buffer (1 M diethanolamine and 0.5 mM magnesium chloride, pH 10.3) was added to the SEAP reporter gene samples and β-galactosidase assay buffer [0.1 M sodium phosphate dibasic, 1 mM magnesium chloride, and 1.4% (v/v) β-mercaptoethanol, pH 7.0] to the β-Galactosidase samples. Fluorescent substrates were added to the wells in the dark, 4-methylumbelliferyl phosphate (2 mM) for SEAP detection or 4-methylumbelliferyl β-galactopyranoside (2 mM) for β-galactosidase detection. Plates were incubated for 1 h at 22°C in the dark then read on the Packard Fusion-Alpha with excitation of the fluorescent substrate at 360 nm and emission at 440 nm.

Confocal Imaging. Cells (5×10^5 cells) were plated onto sterile coverslips (24 × 24 mm) in six-well plates and grown for 2 days at 37°C. The cells were transiently transfected with RXFP3-GFP[2] (500 ng/well) (van der Westhuizen et al., 2009) using Lipofectamine according to the manufacturer's instructions. The growth medium was changed to FBS and antibiotic-free DMEM 18 h before stimulation. The cells were stimulated at 37°C for selected time points then placed on ice. DMEM was aspirated and the cells washed once with ice-cold PBS (pH 7.4), on ice. The cells were fixed with 4% paraformaldehyde (in PBS) for 20 min at 22°C then washed three times with PBS and mounted on glass slides using fluorescent mounting medium (Dako Deutschland GmbH, Hamburg, Germany). Cells were imaged with a laser scanning confocal microscope (TCS-NT inverted microscope; Leica, Mannheim, Germany) using Leica confocal software (ver. 2.5). A Plan Apo 40× (1.25 numerical aperture) oil immersion lens was used for imaging. An argon/krypton/neon laser passed through a short-pass 590 nm filter and a double dichroic 488/568 mirror. The laser was separated into green and red light by a reflective short-pass 580 nm filter with a band-pass 530/30 filter for the green light. The remaining light passed through a band pass 600/30 filter for red light. The airy pinhole was set to 1.00 optical unit. and each image was captured with 512 × 512 pixels in an eight-bit image.

Data and Statistical Analysis. cAMP accumulation assays were normalized against the response to forskolin (30 μM) and ERK1/2 phosphorylation against the response to FBS [10% (v/v)]. SEAP reporter constructs were cotransfected at a 1:1 ratio with constitutively expressed β-galactosidase to account for the variation in transfection efficiency between experiments. SEAP activation was expressed as a percentage of β-galactosidase activation (8 h after cell stimulation) and then normalized against the response to the positive control or the H3 relaxin response. All data are mean ± S.E.M. of n experiments as described in the figure legends.

Competition binding data were simultaneously analyzed for one-site versus two-site competition binding followed by an F test using Prism (ver. 5.0; GraphPad Software, San Diego, CA) to fit the appropriate curve. ERK1/2, NF-κB and AP-1 concentration-response curves were analyzed using a three parameter Hill equation within Prism. cAMP concentration-response curves were analyzed using a four-parameter Hill equation within Prism.

Results

CHO-RXFP3, HEK-RXFP3, and SN56 Cells Do Not Express RXFP1, RXFP2, or RXFP4 mRNA. The profile of RXFPs expressed in CHO-RXFP3, HEK-RXFP3, and SN56 was examined by RT-PCR (Fig. 1) to ensure that any effects observed were mediated solely through RXFP3 receptors. RXFP3 mRNA was detected in CHO-RXFP3, HEK-RXFP3, and SN56 cells but not in CHO-K1, HEK293, HEK-RXFP1, HEK-RXFP2, CHO-RXFP4, or HEK-RXFP4 cells (Fig. 1A). RXFP1 and RXFP2 mRNA expression (Fig. 1B) was detected only in HEK-RXFP1 and HEK-RXFP2 cells and RXFP4 mRNA expression (Fig. 1C) was detected only in CHO-RXFP4 and HEK-RXFP4 cells and not in the other cell lines tested. β-Actin was also amplified as a control to confirm similar levels of cDNA were present in all samples (Fig. 1D). These results show that CHO-RXFP3, HEK-RXFP3, and SN56 cells do not endogenously express other known RXFPs and suggest that any effects of the relaxin family peptides occurs by activation of RXFP3 and not other RXFP receptors.

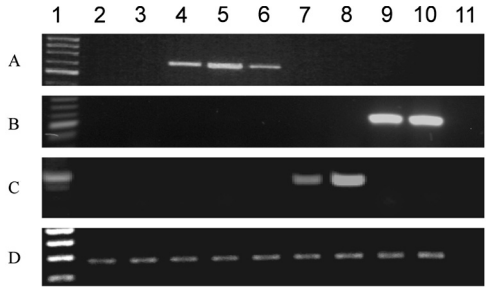

Fig. 1. RXFP1, RXFP2, and RXFP4 mRNA are not present in RXFP3-expressing cells. Expression of RXFP1–4 mRNA in CHO, HEK, and SN56 cell lines was determined using RT-PCR. A, RXFP3 was expressed only in CHO-RXFP3 (lane 4), HEK-RXFP3 (lane 5), and SN56 (lane 6) cells and not in CHO-K1 (lane 2), HEK293 (lane 3), CHO-RXFP4 (lane 7), HEK-RXFP4 (lane 8), HEK-RXFP1 (lane 9), or HEK-RXFP2 (lane 10) cells. B, RXFP1 and RXFP2 were only detected in HEK-RXFP1 and HEK-RXFP2 cells but not in the other cell lines tested. C, RXFP4 was detected only in CHO-K1 and HEK293 cells transiently expressing RXFP4 but not in the other cell lines tested. D, β-actin levels were determined to reflect the amounts of cDNA in each reaction. A 100-base pair molecular size marker (lane 1) was included to determine whether the bands were of the correct size, and a no-cDNA negative control (lane 11) was included to ensure that there was no contaminating DNA present. Data are representative of two experiments, with reverse transcription of each cell line RNA performed in duplicate.

Relaxin Family Peptides Share Regions of Homology with the Predicted Binding Region of H3 Relaxin. Residues Arg8, Arg12, Ile15, Arg16, and Phe20 of H3 relaxin were recently shown to be important for H3 relaxin binding to RXFP3 (Kuei et al., 2007). Alignment of H3 relaxin with H2 relaxin, porcine relaxin, and human INSL3 (Fig. 2), indicated that H2 relaxin, porcine relaxin and human INSL3 each retained homologous resides in all of these positions, except Phe20, suggesting that other relaxin-like peptides may interact with RXFP3. The effects of H2 relaxin, porcine relaxin and INSL3 were tested in parallel with H3 relaxin in RXFP3-expressing cells measuring responses from four different signaling outputs.

ERK1/2 Is Strongly Activated by H3 Relaxin in RXFP3-Expressing Cell Lines. Activation of ERK1/2 was previously demonstrated in CHO-RXFP3, HEK-RXFP3, and SN56 cells after stimulation with H3 relaxin or various H3 relaxin B-chain peptides (van der Westhuizen et al., 2007). Here, we also investigated the effects of H2 relaxin, porcine relaxin, and human INSL3 on this signaling pathway. H3 relaxin (10 nM) strongly activated ERK1/2 in all cell lines with peak ERK1/2 activation [maximum response, 6.57 ± 0.78-fold/basal (CHO-RXFP3); 5.81 ± 1.33-fold/basal (HEK-RXFP3); and 6.55 ± 1.20-fold/basal (SN56)] occurring between 2 and 10 min, consistent with previous results (van der Westhuizen et al., 2007) (n = 6). In addition, H2 relaxin (10 nM) weakly activated ERK1/2 in CHO-RXFP3 (3.12 ± 0.79-fold/basal) and HEK-RXFP3 (1.91 ± 0.29-fold/basal) cells stably expressing human RXFP3 but not in SN56 cells that endogenously express mouse RXFP3. Peak ERK1/2 activa-

```
B-chains:
                          ↓   ↓  ↓↓   ↓
                  1   5     10    15    20    25
porcine relaxin  -QSTNDFIKACGRELVRLWVEICGSVSWGRTAL
H2 relaxin       DSWMEEVIKLCGRELVRAQIAICGMSTWS
H3 relaxin       -RAAPYGVRLCGREFIRAVIFTCGGSRW
INSL3            APTPEMREKLCGHHFVRALVRVCGGPRWSTEARR
                         : **:.::*  :  **   *

A-chains:

                 1   5     10    15    20
porcine relaxin --RMTLSEKCCQVGCIRKDIARLC--
H2 relaxin      QLYSALANKCCHVGCTKRSLARFC--
H3 relaxin      DVLAGLSSSCCKWGCSKSEISSLC--
INSL3           AAATNPARYCCLSGCTQQDLLTLCPY
                      :  **  ** : .:  :*
```

Fig. 2. Clustal W (v1.83) alignment of porcine relaxin, H2 relaxin, H3 relaxin and human INSL3. Full-length porcine relaxin (P01348), human relaxin-2 (P04090), human relaxin-3 (Q8WXF3), and human insulin-like peptide (INSL) 3 (P51460) amino acid sequences were downloaded from the Uniprot/Swissprot database and aligned using Clustal W (ver. 1.83; http://www.ebi.ac.uk/Tools/clustalw2/index.html) with only the A-chain and B-chain peptides shown. Identical amino acid residues between the relaxin peptides are shown by a white letter on a black background. Similar residues in the relaxin peptide sequences are highlighted in gray. * indicates identical amino acid residues in the relaxin peptide and INSL3 sequences; colon (:) or period (.) indicates similarity between the relaxin and INSL3 residues. The arrows above the B-chain residues indicate amino acids that are important for H3 relaxin binding to and activation of RXFP3 (Kuei et al., 2007).

tion to H2 relaxin addition occurred after 5 min and returned to basal after 10 min of stimulation ($n = 6$). Both H3 relaxin [pEC_{50}, 9.18 ± 0.15 (CHO-RXFP3); 9.15 ± 0.13 (HEK-RXFP3); and 9.64 ± 0.27 (SN56)] and H2 relaxin [pEC_{50}, 7.99 ± 0.73 (CHO-RXFP3) and 8.18 ± 0.39 (HEK-RXFP3)] increased ERK1/2 phosphorylation in a concentration-dependent manner (Fig. 3, A, C, and E), and ERK1/2 activation was not observed in untransfected CHO-K1 or HEK293 cells with H3 relaxin, H2 relaxin, porcine relaxin, or INSL3 ($n = 3$; data not shown) in accord with the lack of endogenous expression of RXFP3 in these cells (Fig. 1). These results suggest that H3 relaxin is a full agonist for ERK1/2 phosphorylation in cells that express RXFP3 and that H2 relaxin is a partial agonist at human but not mouse RXFP3.

H3 Relaxin, H2 Relaxin, and Porcine Relaxin Inhibit Forskolin-Stimulated cAMP Accumulation in RXFP3-Expressing Cells. Because RXFP3 was previously shown to inhibit forskolin-stimulated cAMP accumulation in CHO-K1 cells (Liu et al., 2003) and because we also observed weak ERK1/2 activation by H2 relaxin in CHO-RXFP3 and HEK-RXFP3 cells, the effect of these peptides on forskolin-stimulated cAMP accumulation was also investigated. Strong inhibition of forskolin-stimulated [30 μM 3 min (CHO and HEK) or 20 min (SN56)] cAMP accumulation was observed in CHO-RXFP3, HEK-RXFP3, and SN56 cells pretreated with H3 relaxin [pEC_{50}, 9.13 ± 0.10 (CHO-RXFP3); 9.07 ± 0.26 (HEK-RXFP3); and 9.22 ± 0.15 (SN56)], whereas H2 relaxin [pEC_{50}, 7.05 ± 0.15 (CHO-RXFP3); 6.85 ± 0.24 (HEK-RXFP3); and 6.97 ± 0.19 (SN56)] or porcine relaxin [pEC_{50}, 7.30 ± 0.15 (CHO-RXFP3); 7.10 ± 0.22 (HEK-RXFP3); and 7.08 ± 0.22 (SN56)] had much lower potency (Fig. 3, B, D, and F). INSL3 (1 μM) also weakly inhibited forskolin-stimulated cAMP accumulation in CHO-RXFP3 and HEK-RXFP3 [pEC_{50}, 5.77 ± 0.18 (CHO-RXFP3) and 5.81 ± 0.45 (HEK-

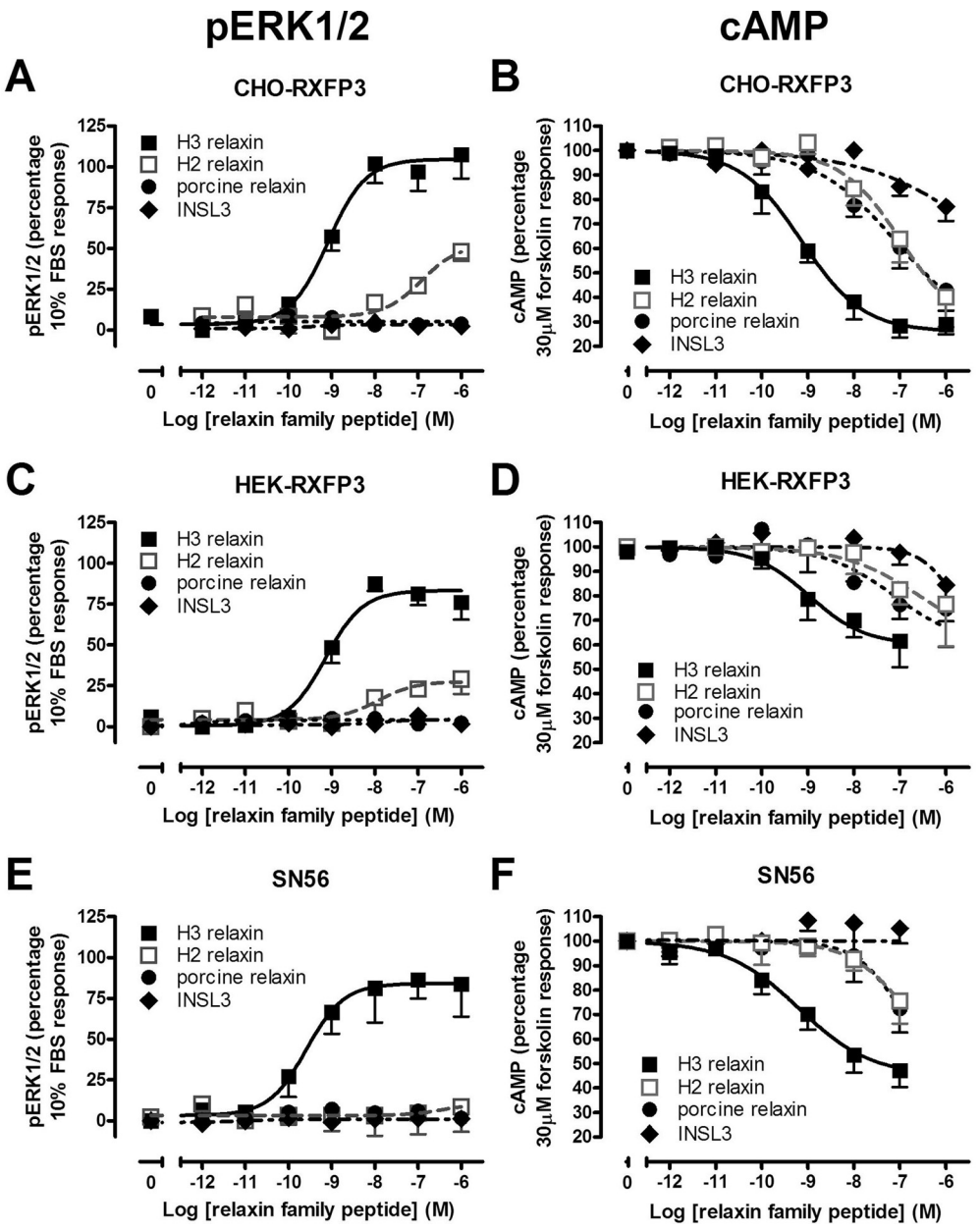

Fig. 3. H3 relaxin potently inhibits forskolin-stimulated cAMP production and activates ERK1/2 in RXFP3-expressing cells. RXFP3-expressing cells were stimulated with relaxin family peptides (range, 1 pM–1 μM) for 5 min at 37°C, then lysed for 16 h at −20°C. Lysates were activated and p-ERK1/2 detected using the AlphaScreen Surefire p-ERK1/2 kit. H3 relaxin potently activated ERK1/2 in CHO-RXFP3 (A), HEK-RXFP3 cells (C), and SN56 cells (E), and H2 relaxin weakly activated ERK1/2 in CHO-RXFP3 and HEK-RXFP3 cells but not in SN56 cells. FBS (10%; 5 min) was used as a positive control [p-ERK1/2 increase fold/basal, 8.87 ± 1.97 (CHO-RXFP3); 10.50 ± 1.43 (HEK-RXFP3); and 7.47 ± 1.23 (SN56)]. Data are normalized and expressed as a percentage of this response. Forskolin-stimulated cAMP accumulation (30 μM) [cAMP pmol/well, 0.83 ± 0.10 (CHO-RXFP3); 0.70 ± 0.05 (HEK-RXFP3); and 1.41 ± 0.18 (SN56)] was inhibited in RXFP3-expressing cells by relaxin family peptides (range, 1 pM–1 μM; 5 min). Potent inhibition of forskolin-stimulated cAMP accumulation was observed in CHO-RXFP3 (B), HEK-RXFP3 (D), andSN56 cells (F) with H3 relaxin [ΔcAMP pmol/well, 0.57 ± 0.05 (CHO-RXFP3); 0.25 ± 0.08 (HEK-RXFP3); and 0.81 ± 0.18 (SN56)]. Although much less potent, H2 relaxin [ΔcAMP pmol/well, 0.54 ± 0.06 (CHO-RXFP3); 0.12 ± 0.07 (HEK-RXFP3); and 0.38 ± 0.21 (SN56)] and porcine relaxin [ΔcAMP pmol/well, 0.49 ± 0.08 (CHO-RXFP3); 0.12 ± 0.01 (HEK-RXFP3); 0.40 ± 0.11 (SN56)] also inhibited forskolin-stimulated cAMP production in all three cell lines. INSL3 [ΔcAMP pmol/well, 0.16 ± 0.16 (CHO-RXFP3) and 0.06 ± 0.02 (HEK-RXFP3)] weakly inhibited forskolin-stimulated cAMP accumulation in CHO-RXFP3 and HEK-RXFP3 cells but not in SN56 cells. The amount of cAMP per well was determined using the AlphaScreen cAMP kit according to a modified protocol (see *Materials and Methods*). Data were expressed as a percentage of the forskolin response. Data are mean ± S.E.M. of six to eight independent experiments with triplicate repeats.

RXFP3)] but not in SN56 cells (Fig. 3, B, D, and F). These results suggest that H2 relaxin, porcine relaxin, and INSL3 can weakly interact with RXFP3 with lower potency than H3 relaxin to inhibit forskolin-stimulated cAMP accumulation. None of the peptides stimulated cAMP accumulation in any of the RXFP3-expressing cell lines after stimulation for 3 to 30 min (data not shown; $n = 3$). This contrasts with the effects of H2 relaxin or INSL3 in HEK293T cells that stably express RXFP1 and RXFP2, respectively (Halls et al., 2005). Taken together, these results suggest that the RXFP3 expressing cells do not express RXFP1 or RXFP2 and that the observed inhibition of forskolin-stimulated cAMP accumulation occurs solely through RXFP3.

AP-1-SEAP and NF-κB-SEAP Reporter Genes Are Activated Downstream of RXFP3. Preliminary screening experiments using eight different *cis*-acting enhancer elements linked to a SEAP reporter gene showed that H3 relaxin stimulation of RXFP3 robustly activated the NF-κB-SEAP and AP-1-SEAP after 4 to 24 h stimulation ($n = 6$; Supplemental Fig. 1). However, surprisingly, H2 relaxin also activated AP-1-SEAP after 4 to 24 h of stimulation to levels equivalent to those observed with H3 relaxin ($n = 6$; Supplemental Fig. 1). No activation of cAMP response element-SEAP, heat shock element-SEAP, nuclear factor of activated T cells-SEAP, E-box DNA binding element-SEAP, glucocorticoid response element-SEAP, or serum response element-SEAP reporter genes was observed in CHO-RXFP3, HEK-RXFP3, and SN56 cells after 4 to 24 h exposure to H3 relaxin, H2 relaxin, or INSL3 (shown for CHO-RXFP3 cells, $n = 6$; Supplemental Fig. 1). All reporter genes were tested with a positive control (forskolin, heat shock, ionomycin, or FBS), confirming that they could be activated in these cells.

The preliminary reporter gene screening suggested that H3 relaxin activated signaling on the NF-κB pathway, whereas H2 relaxin and INSL3 did not ($n = 6$, Supplemental Fig. 1). Subsequent concentration-response analysis demonstrated that H3 relaxin increased activation of NF-κB-SEAP in CHO-RXFP3, HEK-RXFP3, and SN56 cells, with the max-

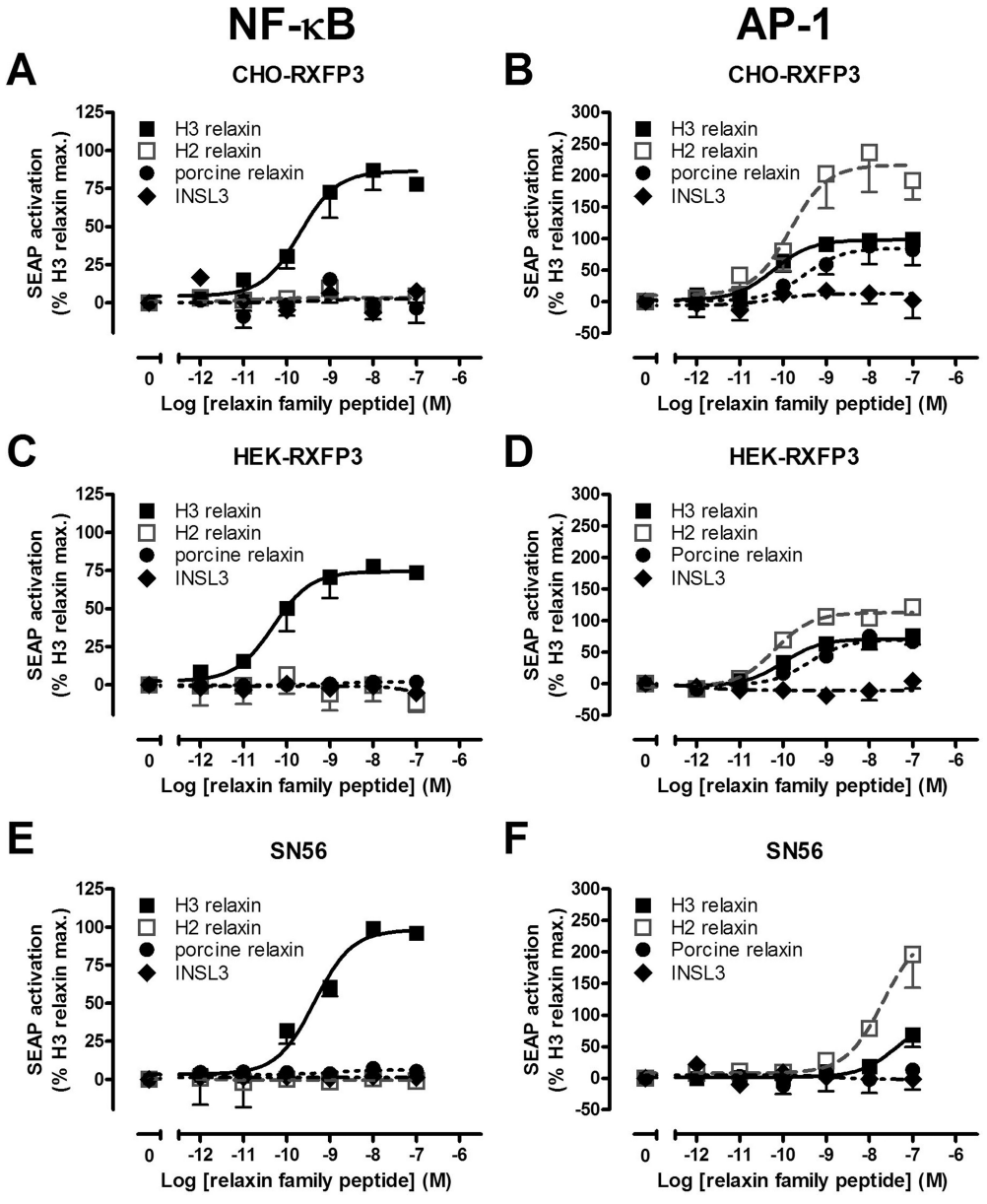

Fig. 4. NF-κB and AP-1 reporter genes are activated by relaxin family peptides. CHO-K1, HEK293, and SN56 cells were transiently cotransfected with RXFP3, NF-κB-SEAP, or AP-1-SEAP reporter genes and a constitutively active β-galactosidase reporter gene. H3 relaxin activated NF-κB reporter genes in CHO-RXFP3 (A), HEK-RXFP3 (C), and SN56 (E) cells, as determined by an increase in SEAP in the culture medium (directly proportional to the increase in transcription from the reporter gene) 8 h after peptide stimulation. NF-κB reporter gene activation (8 h after stimulation) was not observed in cells exposed to H2 relaxin, porcine relaxin, or INSL3. Stimulation with FBS (10%, 8 h) activated NF-κB-SEAP reporter genes in all cell lines [ΔRFU, 2099.00 ± 290.12 (CHO-RXFP3); 2876.80 ± 839.28 (HEK-RXFP3); and 1430.75 ± 376.80 (SN56)]. AP-1 reporter genes were activated in CHO-RXFP3 (B) and HEK-RXFP3 (D) cells with an order of potency H2 relaxin > H3 relaxin > porcine relaxin 4 h after peptide stimulation. A similar pattern was observed in SN56 cells (F), although the pEC_{50} was shifted to the right compared with CHO-RXFP3 and HEK-RXFP3. FBS (10%; 8 h) was used as a positive control in all cell lines to demonstrate that the reporter genes were functional in the cells [ΔRFU, 805.96 ± 87.55 (CHO-RXFP3); 237.17 ± 38.65 (HEK-RXFP3); and 3211.97 ± 230.66 (SN56)] No AP-1 reporter gene activation was observed in cells exposed to INSL3. Data were expressed as a percentage of β-galactosidase activation (8 h after peptide stimulation) [RFU, 20,217.97 ± 3604.03 (CHO-RXFP3); 25,491.94 (HEK-RXFP3); and 481.35 ± 26.22 (SN56)] and then normalized to the maximum H3 relaxin response. Data are mean ± S.E.M. of six independent experiments with each point determined in duplicate.

imum response observed at 10 nM (Fig. 4, A, C, and E) [ΔRFU, 1074.50 ± 69.28 (CHO-RXFP3); 1076.50 ± 349.84 (HEK-RXFP3); and 555.70 ± 181.27 (SN56)]. Activation of NF-κB-linked reporter genes were not observed in the same cells treated with H2 relaxin, porcine relaxin, or INSL3 (Fig. 4, A, C, and E) or in CHO-K1 or HEK293 cells expressing NF-κB reporter genes but not RXFP3 receptors when exposed to H3 relaxin, H2 relaxin, porcine relaxin, or INSL3 ($n = 3$; data not shown). The H3 relaxin-mediated increase in NF-κB reporter gene activation was blocked in cells pretreated with PTX (100 ng/ml) (Fig, 5, B, D, and F), suggesting that the NF-κB signaling pathway was activated downstream of PTX-sensitive $G\alpha_{i/o}$ proteins.

The preliminary reporter gene screening experiments also indicated that RXFP3 activated signaling in pathways leading to increased transcription from AP-1 sites (Supplemental Fig. 1). In contrast to the NF-κB reporter gene assays, H2 relaxin [ΔRFU, 641.17 ± 14.44 (CHO-RXFP3) and 228.12 ± 46.50 (HEK-RXFP3)], porcine relaxin [ΔRFU, 261.33 ± 139.85 (CHO-RXFP3) and 176.42 ± 67.52 (HEK-RXFP3)], as well as H3 relaxin, [ΔRFU, 299.14 ± 86.06 (CHO-RXFP3) and 133.33 ± 28.86 (HEK-RXFP3)] increased activation of AP-1-linked reporter genes in a concentration-dependent manner in CHO-RXFP3 and HEK-RXFP3 cells (Fig. 4, B and D; Table 1). H2 relaxin [ΔRFU, 4029.62 ± 486.12] and H3 relaxin [ΔRFU, 1173.17 ± 143.42] also activated AP-1-linked reporter genes expressed in SN56 cells (Fig. 4F), although the potencies of H2 relaxin and H3 relaxin were lower than in CHO-RXFP3 and HEK-RXFP3 cells (Table 1). However, the relative potency and efficacy (i.e., H2 relaxin > H3 relaxin) was similar in all cell lines. Porcine relaxin did not activate AP-1-linked reporter genes in SN56 cells and INSL3 did not activate the reporter in any of the cells. No AP-1 reporter gene activation was observed in CHO-K1 or HEK293 cells expressing AP-1 reporter genes but not RXFP3, after treatment with H3 relaxin, H2 relaxin, porcine relaxin, or INSL3 ($n = 3$; data not shown), again suggesting that the relaxin family peptides activated the AP-1-linked reporter gene solely through RXFP3.

In all cell lines, AP-1 reporter gene activation by H2 relaxin was blocked by pretreatment with PTX (100 ng/ml) (Fig. 5, A, C, and E), suggesting that the signaling pathways involved in increased gene transcription from AP-1 sites were activated downstream of PTX-sensitive $G\alpha_{i/o}$ proteins. In contrast, AP-1 reporter gene activation by H3 relaxin [ΔRFU, 870.50 ± 268.65 (CHO-RXFP3); 154.85 ± 37.45 (HEK-RXFP3); and 83.80 ± 21.14 (SN56)] was not blocked in CHO-RXFP3 or HEK-RXFP3 cells pretreated with PTX (Fig. 5, A and C) [ΔRFU, 892.56 ± 189.34 (CHO-RXFP3) and 144.80 ± 36.67 (HEK-RXFP3)], although the same treatment blocked the response to H3 relaxin in SN56 cells (Fig. 5E) (ΔRFU, −29.17 ± 25.26), suggesting that differential compartmentalization of RXFP3 in the different cell backgrounds influences the ability to couple to $G\alpha_{i/o}$ proteins. The results also indicate that H3 relaxin and possibly porcine relaxin use a $G\alpha_{i/o}$ protein-independent mechanism to activate AP-1 reporter genes in CHO-RXFP3 and HEK-RXFP3 cells. AP-1 reporter gene activation ± PTX and NF-κB ± PTX experiments were performed in parallel, suggesting that the PTX used in these experiments was active and could block responses downstream of RXFP3.

TABLE 1

pEC_{50} values for H3 relaxin, H2 relaxin, porcine relaxin, and INSL3 activation of AP-1 reporter genes in RXFP3-expressing cell lines

Cells	H3 Relaxin	H2 Relaxin	Porcine Relaxin	INSL3
CHO-RXFP3	10.3 ± 0.24	9.92 ± 0.25	9.52 ± 0.35	N.A.
HEK-RXFP3	9.93 ± 0.20	10.1 ± 0.18	9.32 ± 0.21	N.A.
SN56	7.37 ± 0.39	7.68 ± 0.25	N.A.	N.A.

N.A., no activation.

Identification of Two Binding Sites in RXFP3-Expressing Cell Lines with the Use of ^{125}I-INSL5/H3 Relaxin Chimera or ^{125}I-H2 Relaxin. To determine the binding profile of the relaxin family peptides in CHO-RXFP3, HEK-RXFP3, and SN56 cells, competition for ^{125}I-INSL5/H3 relaxin chimera binding was assessed. ^{125}I-INSL5/H3 relaxin is a high-affinity selective ligand for RXFP3 and RXFP4 (Liu et al., 2005) used previously to characterize RXFP3 expressed in COS-7, CHO-K1, or HEK293 cells (Liu et al., 2005; van der Westhuizen et al., 2007). Competition for ^{125}I-INSL5/H3 relaxin binding in CHO-RXFP3, HEK-RXFP3, and SN56 cells was observed with H3 relaxin, [pK_i = 9.02 ± 0.15 (CHO-RXFP3); 9.20 ± 0.18 (HEK-RXFP3); and 8.52 ± 0.05 (SN56)]. H2 relaxin, porcine relaxin, or human INSL3 did not compete for binding at this site at concentrations up to 1 μM (Fig. 6, A, C, and E). No specific ^{125}I-INSL5/H3 relaxin binding was observed in untransfected CHO-K1 or HEK293 cells ($n = 3$; data not shown).

To examine whether these potent effects of the relaxins could be mediated by interaction with a distinct RXFP3 binding site that could be recognized by H2 relaxin with high affinity, ^{125}I-H2 relaxin was used to determine specific binding at RXFP3 (Fig. 6, B, D, and F; Table 2). Specific ^{125}I-H2 relaxin binding was observed on HEK-RXFP1 cells (pIC_{50}, 7.87 ± 0.10) but not in untransfected CHO-K1 or HEK293 cells ($n = 3$; data not shown). Potent competition for ^{125}I-H2 relaxin binding was observed in CHO-RXFP3 and HEK-RXFP3 cells with H3 relaxin, H2 relaxin, and INSL3, with weak competition by porcine relaxin (Fig. 6, B and D; Table 2). A slightly different profile was observed in SN56 cells, where competition for ^{125}I-H2 relaxin binding was observed with H3 relaxin > H2 relaxin > porcine relaxin ≫ INSL3 (Fig. 6F). The number of H2 relaxin binding sites (B_{max}) was calculated from the H2 relaxin competition binding curves (Table 2). There were 3-fold (CHO-RXFP3), 7.5-fold (HEK-RXFP3), or 13-fold (SN56) more INSL5/H3 relaxin binding sites than H2 relaxin binding sites. These results may suggest that the ligands select different receptor conformations that exist in different proportions in different cell systems.

INSL3 Does Not Functionally Antagonize the ERK1/2 or AP-1 Reporter Gene Signaling Pathway. Because INSL3 had weak effects at RXFP3 for inhibition of forskolin-stimulated cAMP accumulation, a ^{125}I-INSL3 binding site was also sought on RXFP3-expressing cells. Specific ^{125}I-INSL3 binding was observed on HEK-RXFP2 cells (pIC_{50}, 8.97 ± 0.12), but no ^{125}I-INSL3 binding was detected on RXFP3-expressing cells ($n = 3$–6, data not shown). To determine whether there is any functional interaction between INSL3 and RXFP3, the effect of INSL3 on either the H3 relaxin (10 nM) response in ERK1/2 activation and its effect on AP-1 reporter gene activation mediated by H2 or H3 relaxin (10 nM) were examined. Increasing concentrations of INSL3 did not affect ERK1/2 activation by H3 relaxin (10 nM) in CHO-RXFP3, HEK-RXFP3, or SN56

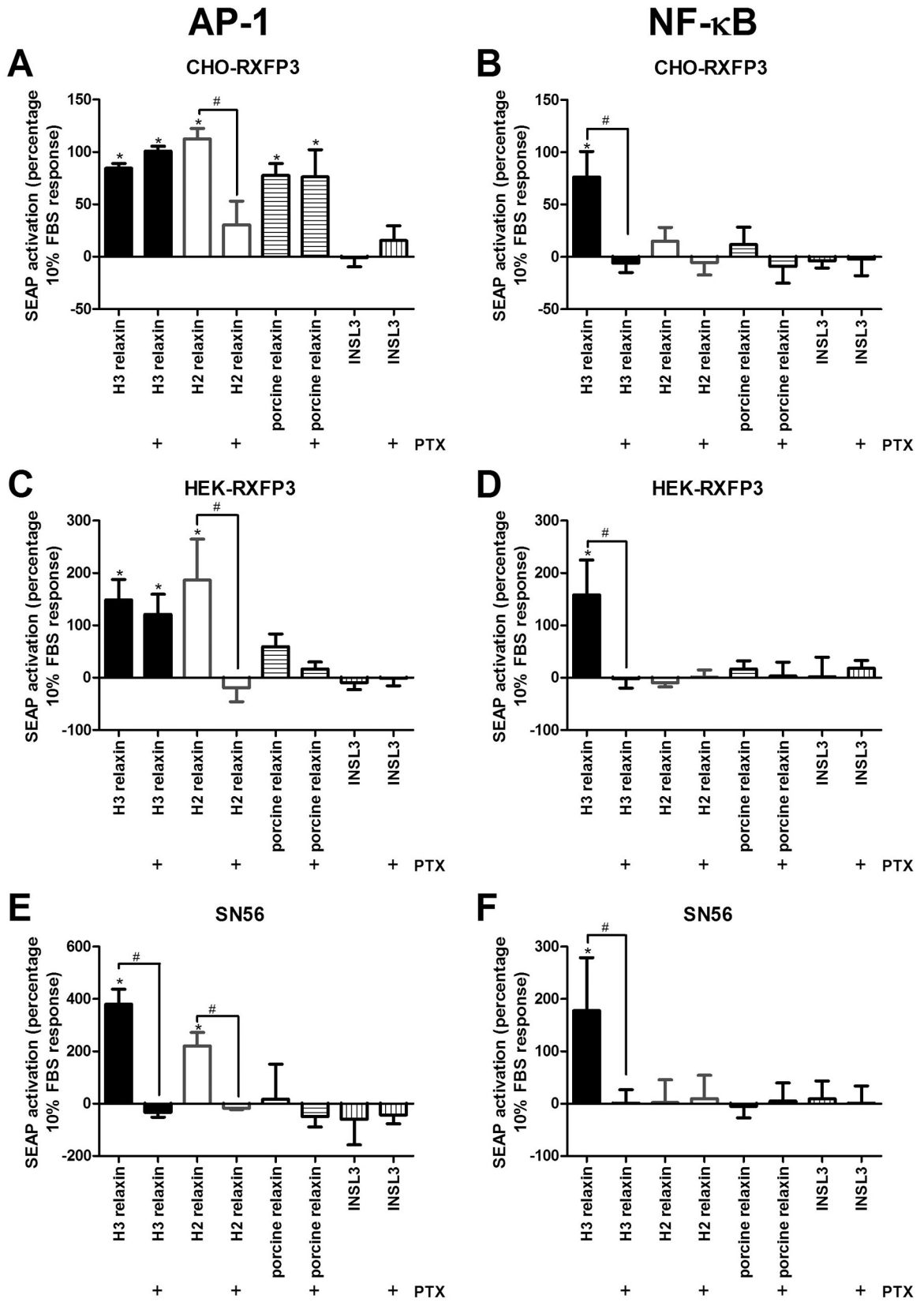

Fig. 5. $G\alpha_{i/o}$ proteins are involved in AP-1 and NF-κB reporter gene activation in a cell type- and peptide-dependent manner. AP-1 reporter gene activation (4 h; 37°C) stimulated by H3 relaxin and porcine relaxin (both 10 nM) was not blocked in CHO-RXFP3 (A) or HEK-RXFP3 (C) cells, expressing human RXFP3 receptors and pretreated with PTX (100 ng/ml; 18 h). The H3 relaxin-mediated response (ΔRFU, 83.8 ± 21.14) was blocked by PTX (ΔRFU, −29.16 ± 25.26) in SN56 cells (E) expressing mouse RXFP3 receptors. Porcine relaxin did not activate AP-1 reporter genes in SN56 cells (E). H2 relaxin (10 nM) stimulated AP-1 reporter gene activation (4 h; 37°C) [ΔRFU, 66.70 ± 20.83 (SN56)]was blocked in PTX pretreated CHO-RXFP3 (A), HEK-RXFP3 (C), and SN56 cells (E) (ΔRFU, −33.83 ± 20.28). INSL3 did not activate AP-1 reporter genes in any cell line tested.

cells ($n = 3$, data not shown) or AP-1 reporter gene activation by H3 relaxin (10 nM) or H2 relaxin (10 nM) in any cell line tested ($n = 6$; data not shown), suggesting that INSL3 does not act as a functional antagonist for either pathway.

AP-1 Reporter Gene Activation Occurs Downstream of p38 MAPK, c-Jun N-Terminal Kinase, and ERK Signaling Pathways in a Cell Line- and Peptide-Dependent Manner. To determine which signaling pathways were activated downstream of RXFP3 but upstream of AP-1 reporter genes in CHO-RXFP3, HEK-RXFP3, and SN56 cells by H2 relaxin, H3 relaxin, and porcine relaxin, a pharmacological inhibitor approach was employed. It is known that gene transcription from AP-1 sites may occur downstream of the p38 MAPK, JNK, ERK1/2, or ERK5 signaling pathways (Price et al., 1996; Whitmarsh and Davis, 1996; Roux and Blenis, 2004). Therefore, AP-1 reporter gene activation was investigated in cells pretreated with inhibitors of these signaling pathways. H3 relaxin-mediated AP-1 reporter gene activation was completely blocked in CHO-RXFP3 cells pretreated with the p38 MAPK inhibitor, RWJ67657 (10 μM; 30 min), at all concentrations of H3 relaxin tested (1 pM-0.1 μM; 4 h) (Fig. 7A), suggesting that p38 MAPK was important for H3 relaxin-mediated AP-1 activation in these cells. Pretreatment of CHO-RXFP3 cells with the MEK inhibitor PD98059 (20 μM; 30 min) or with the JNK inhibitor SP600125 (10 μM; 30 min) shifted the H3 relaxin concentration-response curve to the right, suggesting that ERK and JNK also have roles in H3 relaxin-mediated AP-1 activation in CHO-RXFP3 cells (Fig. 7A).

H2 relaxin-mediated AP-1 activation was strongly attenuated in CHO-RXFP3 cells pretreated with RWJ67657 and SP600125 (Fig. 7B), and PD98059 pretreatment shifted the pEC_{50} of the concentration-response curve to the right without decreasing the maximum response (Fig. 7B). This suggested that both p38 MAPK and JNK play a dominant role in

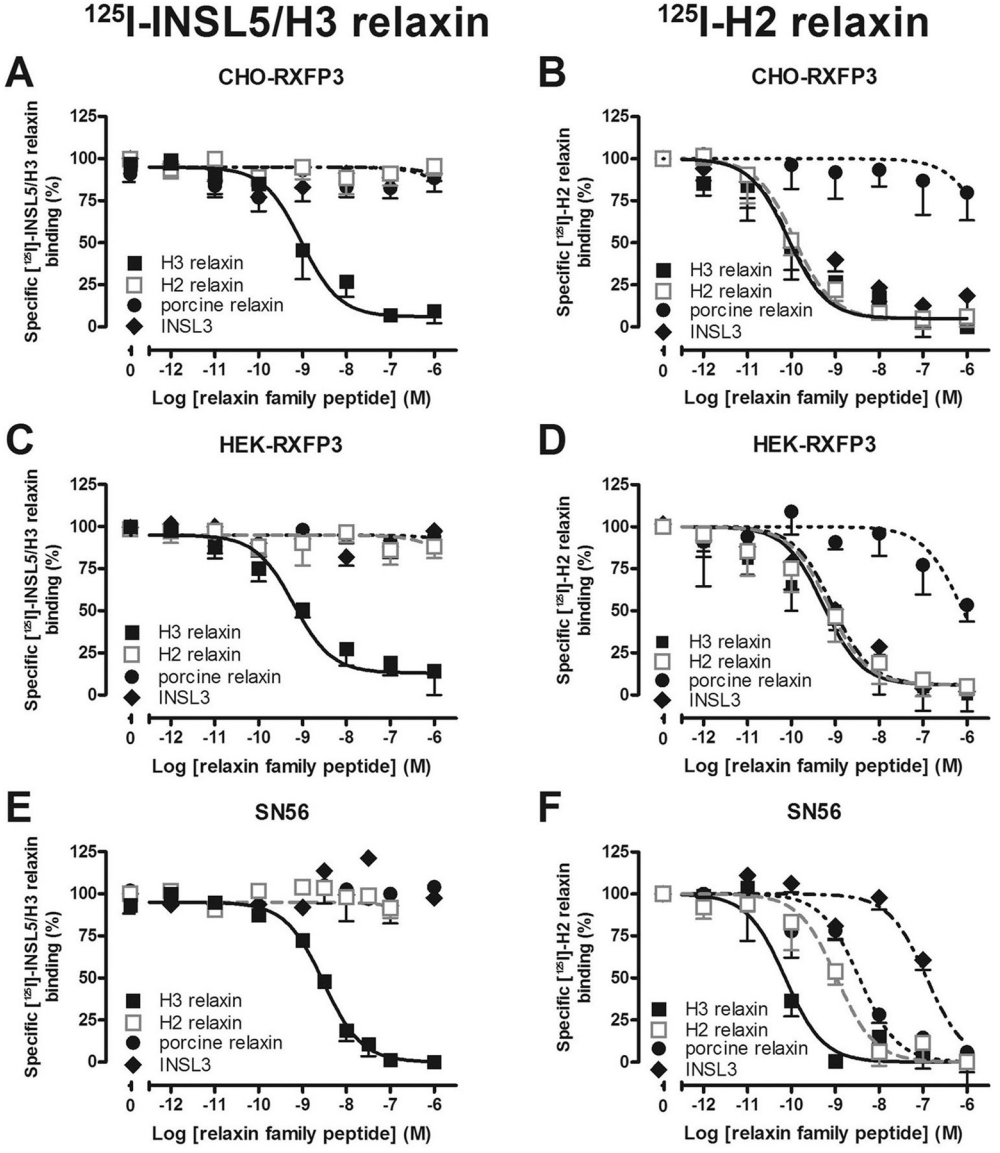

Fig. 6. Characterization of binding sites on RXFP3 using ^{125}I-INSL5/H3 relaxin and ^{125}I-H2 relaxin. Competition for ^{125}I-INSL5/H3 relaxin chimera (100 pM) binding was observed with H3 relaxin in CHO-RXFP3 (A), HEK-RXFP3 (C), and SN56 cells (E). No competition was observed with H2 relaxin, porcine relaxin, or INSL3. Nonspecific binding was defined in the presence of H3 relaxin (1 μM) [specific cpm bound, 2064.18 ± 1447.87 (CHO-RXFP3); 1506.75 ± 405.45 (HEK-RXFP3); and 3967.11 ± 1662.77 (SN56)]. Competition for ^{125}I-H2 relaxin binding was observed in CHO-RXFP3 (B) and HEK-RXFP3 (D) cells. H2 relaxin, H3 relaxin, and INSL3 all competed for binding at this site, with weaker competition observed with porcine relaxin. However, a different competition binding profile was observed in SN56 cells (F), where H3 relaxin was the most potent competitor for ^{125}I-H2 relaxin binding, followed by H2 relaxin and porcine relaxin, and weaker competition was observed with INSL3. Nonspecific binding was defined in the presence of H2 relaxin (1 μM) [specific cpm bound, 5652.99 ± 1943.27 (HEK-RXFP1); 2163.41 ± 712.35 (CHO-RXFP3); 1250.39 ± 544.11 (HEK-RXFP3); and 4568.84 ± 1625.84 (SN56)]. Data are mean ± S.E.M. of six independent experiments, conducted in duplicate.

H3 relaxin-mediated NF-κB reporter gene activation (8 h; 37°C) was blocked by PTX pretreatment in CHO-RXFP3 (B), HEK-RXFP3 (D), and SN56 cells (F). No other relaxin family peptide tested activated NF-κB, and there was no change in cells pretreated with PTX. Data are mean ± S.E.M. of eight independent experiments with each point determined in duplicate.

H2 relaxin-mediated AP-1 activation and that ERK has a minor role.

Porcine relaxin-activated transcription from AP-1 elements was blocked in CHO-RXFP3 cells pretreated with SP600125 (Fig. 7C), suggesting that the JNK signaling pathway was important for AP-1 activation. PD98059 or RWJ67657 pretreatment shifted the pEC_{50} of the porcine relaxin concentration-response curve to the right (Fig. 7C) suggesting that both p38 MAPK and ERK also influence transcription from AP-1 elements in CHO-RXFP3 cells. Together the results with relaxin family peptides suggested that combinations of pathways are required for maximum AP-1 reporter gene activation with some variation observed downstream of receptor activation by the different peptides.

TABLE 2

pIC_{50} values for H3 relaxin, H2 relaxin, porcine relaxin, and INSL3 at the ^{125}I-H2 relaxin binding site

Cells	H3 Relaxin	H2 Relaxin	Porcine Relaxin	INSL3
CHO-RXFP3	10.1 ± 0.19	10.0 ± 0.11	5.49 ± 0.29	10.1 ± 0.17
HEK-RXFP3	9.12 ± 0.16	9.22 ± 0.20	6.11 ± 0.21	9.04 ± 0.18
SN56	10.1 ± 0.13	8.97 ± 0.10	8.45 ± 0.21	6.92 ± 0.22

Pretreatment of HEK-RXFP3 cells with SP600125 completely blocked AP-1 activation at all concentrations of H3 relaxin tested (Fig. 7D), suggesting that JNK was mandatory for H3 relaxin-mediated AP-1 activation. Pretreatment of cells with either PD98059 or RWJ67657 shifted the H3 relaxin concentration-response curve to the right, suggesting that ERK and p38 MAPK pathways were also involved. H2 relaxin-mediated AP-1 activation was strongly attenuated in HEK-RXFP3 cells pretreated with PD98059 and RWJ67657 (Fig. 7E). This suggests that both p38 MAPK and ERK are important in H2 relaxin-mediated AP-1 activation in HEK-RXFP3 cells. In contrast, SP600125 pretreatment did not alter the H2 relaxin concentration-response curve, suggesting that the JNK signaling pathway is not involved.

Porcine relaxin-mediated AP-1 activation was blocked by RWJ67657 and PD98059 in HEK-RXFP3 cells (Fig. 7F), suggesting that p38 MAPK and ERK were important for AP-1

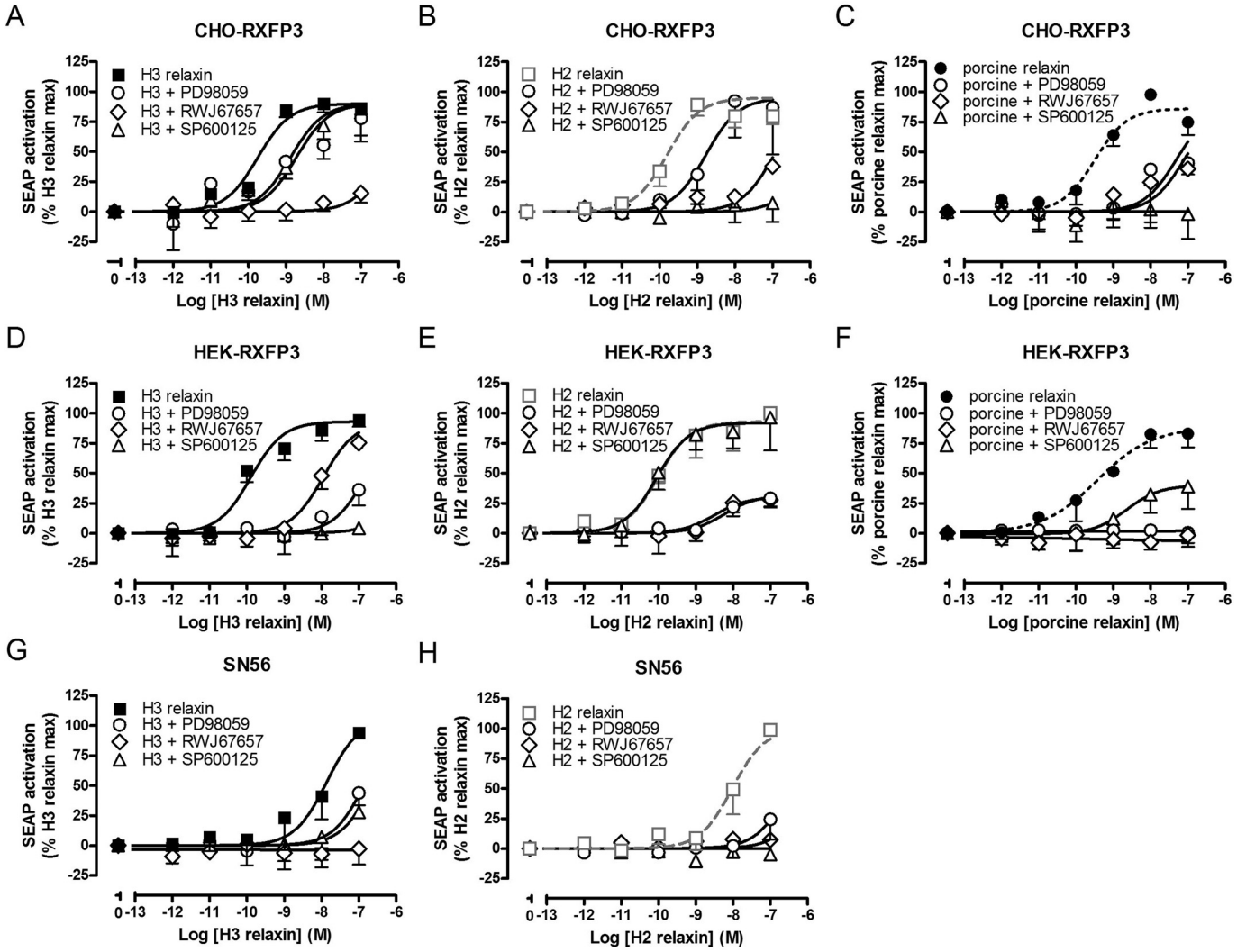

Fig. 7. Several MAPKs are important in activating AP-1 reporter genes in CHO-K1, HEK293, and SN56 cells after relaxin family peptide stimulation. AP-1 reporter genes were activated in CHO-K1 cells after stimulation with H3 relaxin (A), H2 relaxin (B), and porcine relaxin (C). AP-1 reporter genes were also activated in HEK293 cells after stimulation with H3 relaxin (D), H2 relaxin (E), and porcine relaxin (F) and in SN56 cells stimulated with H3 relaxin (G) and H2 relaxin (H). The responses to these peptides were differentially inhibited by PD98059 (20 μM; MEK1/2/MEK5), RWJ67657 (10 μM; p38 MAPK), and SP600125 (10 μM; JNK). Cells were pretreated with inhibitors (30 min), and the inhibitors remained in the medium for the duration of the experiment (4 h). Data are mean ± S.E.M. of eight individual experiments with repeats in duplicate.

reporter gene activation. Porcine relaxin did not activate ERK1/2 in HEK-RXFP3 cells (Fig. 3D), so it is unlikely that PD98059 produces this effect by blockade of MEK1/2. Because PD98059 also inhibits MEK5 at concentrations similar to those that inhibit MEK1/2, it is likely that the inhibition results from its effect on this pathway (Kamakura et al., 1999). In contrast, SP600125 treatment only partially abrogated the response (39.80 ± 14.66%; Fig. 7F).

Pretreatment of SN56 cells with RWJ67657 completely blocked AP-1 activation at all concentrations of H3 relaxin tested (Fig. 7G), suggesting that p38 MAPK was mandatory for H3 relaxin-mediated AP-1 activation. Pretreatment with PD98059 or SP600125 partially blocked AP-1 activation, suggesting that ERK and JNK were also involved. Inhibition of one MAPK signaling pathway did not always completely inhibit the responses to relaxin family peptides, suggesting that in the absence of one MAPK pathway, other MAPK pathways may be able to compensate (Fig. 7G). H2 relaxin-mediated AP-1 activation was blocked in SN56 cells pretreated with SP600125, PD98059, and RWJ67657 (Fig. 7H), suggesting that ERK, JNK, and p38 MAPK were all equally important for AP-1 activation in these cells. However, analysis was limited by the amount of peptides that could be synthesized, which did not allow full concentration-response curves to be constructed.

Internalization of RXFP3 Occurred after Stimulation with H3 Relaxin, but Not H2 Relaxin, Porcine Relaxin, or INSL3. To determine whether H2 relaxin, porcine relaxin, or INSL3 influenced RXFP3 trafficking, agonist-dependent receptor internalization was assessed. The number of cell surface ^{125}I-INSL5/H3 relaxin binding sites was reduced in CHO-RXFP3, HEK-RXFP3, or SN56 cells after stimulation with H3 relaxin (0.1 μM) (Fig. 8, A–C), consistent with RXFP3 internalization. However, the number of cell-surface binding sites was not reduced in cells exposed to H2 relaxin, porcine relaxin, or INSL3 (all 0.1 μM) (Fig. 8, A–C), suggesting that these ligands do not cause RXFP3 internalization. In fact, H2 relaxin (but not porcine relaxin or INSL3) seemed to increase the number of cell-surface binding sites in CHO-RXFP3 cells (Fig. 8A) but not significantly in HEK-RXFP3 or SN56 cells (Fig. 8, B and C).

RXFP3 tagged with GFP^2 at its C-terminal tail was transiently expressed and used to visualize internalization in CHO-K1 and HEK293 cells after 60-min exposure to H3 relaxin, H2 relaxin, porcine relaxin, or INSL3. Similar images were obtained in both cell lines; only the images from HEK293 cells are shown here. RXFP3-GFP^2 was expressed at the cell surface in unstimulated cells (Fig. 8D) and treatment with vehicle (0.001% TFA) did not alter the distribution (Fig. 8D). After stimulation with H3 relaxin (10 nM, 60 min), RXFP3-GFP^2 internalized into small vesicle-like structures (Fig. 8D), but this did not occur in cells treated with H2 relaxin, porcine relaxin, or INSL3 (Fig. 8D). The images obtained by confocal microscopy were consistent with the results of the internalization binding studies (Fig. 8B), suggesting that only H3 relaxin causes RXFP3 internalization. However, the apparent increase in ^{125}I-INSL5/H3 relaxin binding sites by H2 relaxin treatment of CHO-RXFP3 cells was not observed in the confocal imaging studies.

Discussion

RXFP3 is a G$\alpha_{i/o}$-coupled receptor that inhibits forskolin-stimulated cAMP accumulation (Liu et al., 2003) and activates ERK1/2 (van der Westhuizen et al., 2007) after stimulation with H3 relaxin. This study identifies previously unrecognized signaling pathways activated by RXFP3, after H3 relaxin stimulation (i.e., the NF-κB pathway and several signaling pathways that converge on AP-1 transcription sites). Moreover, activation of AP-1 transcription revealed novel interactions of RXFP3 with H2 relaxin, porcine relaxin, and INSL3.

An emerging paradigm in GPCR pharmacology is the selective stabilization of different receptor conformations by ligands, resulting in selective activation of downstream signal transduction pathways (Kenakin, 2003; for review, see Baker and Hill, 2007). This study demonstrates that several relaxin family peptides interact with RXFP3 and activate signaling through different and sometimes overlapping pathways. H3 relaxin was the most potent activator of signaling pathways downstream of RXFP3; however, H2 relaxin was more efficacious in activating transcription of AP-1 reporter genes. It has been reported that porcine relaxin and INSL3 do not inhibit forskolin-stimulated cAMP accumulation in RXFP3-expressing cells (Liu et al., 2003), which differs from the findings here. The experimental conditions used here (37°C, 30 μM forskolin, 3 min) differ from those in the earlier study (23°C, 5 μM forskolin, 25 min), which may increase the signal window and enable observation of weak H2 relaxin, porcine relaxin, and INSL3 inhibition of the cAMP response.

Inhibition of the H3 relaxin-mediated ERK1/2 and NF-κB responses and H2 relaxin-mediated AP-1 response by PTX suggest that these pathways are downstream of G$\alpha_{i/o}$ and that GTPγS binding should be observed for both ligands. However, increases in GTPγS binding were not observed after porcine relaxin or INSL3 (Liu et al., 2003). Because membranes are made before ligand stimulation, movement of RXFP3 between membrane compartments may be prevented, thus restricting receptor conformations available and possibly excluding those that bind H2 relaxin. For instance, the oxytocin receptor is G$\alpha_{i/o}$-coupled in membrane rafts, but after activation it abandons the rafts and becomes Gα_q-coupled (Chini and Parenti, 2004). Therefore, if the H3 relaxin binding conformation of RXFP3 is localized to membrane rafts, it may move out of these regions after activation by H3 relaxin and develop a conformation that recognizes H2 relaxin, porcine relaxin, or INSL3. This behavior may not be observed in GTPγS binding assays with membranes made before receptor stimulation. Alternatively, activation of signaling in RXFP3-expressing cells by H2 relaxin, porcine relaxin, and INSL3 could occur via endogenous expression of low levels of other RXFPs. However, H2 relaxin, H3 relaxin, or INSL3 do not activate AP-1 reporter genes in HEK-RXFP1 cells (Halls et al., 2007), suggesting that the activation of transcription from AP-1 sites observed in CHO-RXFP3 and HEK-RXFP3 cells occurs downstream of RXFP3 and not RXFP1. In addition, because no RXFP1, RXFP2, or RXFP4 mRNA was expressed in the RXFP3-cell lines, this seems an unlikely explanation for the H2 relaxin-mediated activation of AP-1 reporter genes.

Transcription from AP-1 sites can occur via JNK (Davis, 2000), p38 MAPK (Roux and Blenis, 2004), ERK1/2 (Whit-

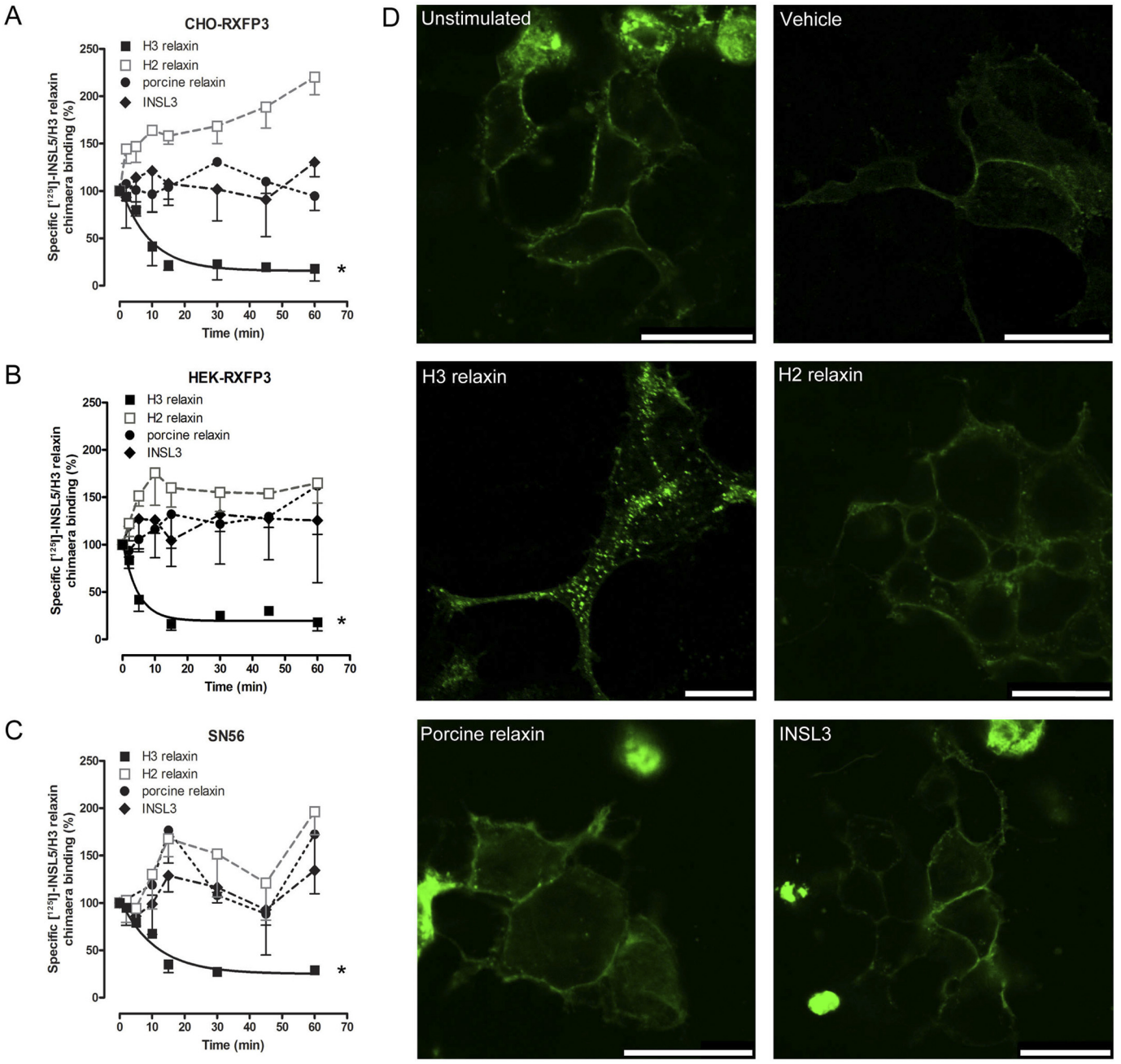

Fig. 8. RXFP3 is internalized after treatment with H3 relaxin, but not with H2 relaxin, porcine relaxin, or INSL3. Stimulation of CHO-RXFP3 cells (A), HEK-RXFP3 cells (B), or SN56 cells (C) with H3 relaxin (10 nM) reduced the number of cell surface ^{125}I-INSL5/H3 relaxin binding sites (as determined by binding on ice for 4 h). No internalization was observed in cells treated with H2 relaxin, porcine relaxin or INSL3 (all 10 nM). Data are mean ± S.E.M. of six independent experiments with repeats in duplicate. Data were analyzed by one-way analysis of variance with a Bonferroni post hoc test to compare all data sets; *, $p < 0.05$ versus INSL3. Internalization of RXFP3-GFP[2] was also visualized in HEK293 cells (D) by confocal imaging, confirming that RXFP3 was expressed at the cell surface of unstimulated cells and internalized in cells treated with H3 relaxin (10 nM; 60 min) but not in cells stimulated with vehicle (0.0001% TFA), H2 relaxin, porcine relaxin, or INSL3 (all 10 nM; 60 min). Data are representative images from four independent experiments, where six different frames were imaged for each treatment in each experiment.

marsh and Davis, 1996), and/or ERK5 (Price et al., 1996) by regulation of c-Jun, c-Fos, MEF-2, and ATF2 (Price et al., 1996; Marinissen et al., 1999; Roux and Blenis, 2004). Examination of the patterns of RXFP3-mediated responses with ERK, JNK, and p38 MAPK inhibitors, suggested that the AP-1 reporter genes were activated by a combination of MAPK pathways. The hierarchy of the different signaling pathways involved in AP-1 reporter gene activation varied with the cell background and with the stimulating peptide, such that p38 MAPK was most important in CHO-RXFP3 cells with H3 relaxin, HEK-RXFP3 cells with H2 or porcine relaxin, and in SN56 cells with H3 or H2 relaxin. JNK was more important in CHO-RXFP3 cells stimulated with H2 or porcine relaxin, in HEK-RXFP3 cells with H3 relaxin, and in SN56 cells with H2 relaxin. Because activation of transcription from AP-1 sites is a complex process involving integration of many MAPKs, significant signal amplification of AP-1 reporter gene activation may occur after weak activation of one or more of the pathways (Marinissen et al., 1999), so weak activation of ERK1/2 by H2 relaxin in CHO-RXFP3 and

HEK-RXFP3 cells may contribute to activation of transcription from AP-1 sites. Activation of transcription may be functionally relevant because dramatic increases in phosphorylated MEK1/2, MKK4, ERK1/2, JNK1, JNK2, and JNK3 are observed immediately after forced swim tests in rats, suggesting that ERK1/2 and JNK are important in stress responses (Shen et al., 2004). H3 relaxin mRNA is also increased in the nucleus incertus after forced swim tests (Tanaka et al., 2005) and probably activates RXFP3 and MAPK signaling, although direct activation of MAPK in the brain by relaxin family peptides remains to be demonstrated.

The inhibitors selected to investigate the signaling pathways involved in AP-1 reporter gene activation downstream of RXFP3 were PD98059 (MEK1/2, MEK5), SP600125 (JNK1/2/3), and RWJ67657 (p38α/p38β MAPK), which have been tested for cross-reactivity against the other MAPKs (Wadsworth et al., 1999; Davies et al., 2000; Bain et al., 2007). PD98059 inhibits MEK1/2 (Alessi et al., 1995) but also MEK5 (Kamakura et al., 1999). Tested in vitro against a panel of protein kinases, it did not inhibit JNK1, ERK2, or p38 MAPK at concentrations that inhibit MEK1/2/5 in cell-based assays (Davies et al., 2000). SP600125 potently inhibits JNK1/2 and JNK3, but not p38 MAPK or ERK1/2, although it partially inhibits MEK1 (Bain et al., 2007). RWJ67657 is a p38α/p38β MAPK inhibitor (Wadsworth et al., 1999) that is more potent than SB203580 and does not inhibit ERK2 (Wadsworth et al., 1999; Bain et al., 2007). SB203580 also inhibits JNK2/3 activity (40% inhibition) (Bain et al., 2007), as may RWJ67657, although this remains to be tested. In HEK293 cells stimulated with H2 relaxin, SP600125 had no effect on AP-1 activation, whereas in CHO-K1 cells, the response to H2 relaxin was blocked, suggesting selectivity of SP600125 against its intended kinase. Likewise, RWJ67657 blocked H3 relaxin-mediated AP-1 activation in CHO-K1 cells, but inhibition was less in HEK293 cells, and PD98059 partially inhibited H2 relaxin-mediated AP-1 activation in HEK293 cells but was a less effective inhibitor of H3 relaxin-mediated responses. This study poses the question "What other MAPKs are activated downstream of RXFP3?"; thus, experiments to confirm that relaxin-family peptides directly activate ERK5, p38 MAPK, or JNK, and the effects of PD98059, SP600125 and RWJ67657, would be relevant to the results presented here.

Significant cross-talk also occurs between MAPKs at the level of protein kinase C (PKC), Raf/Rac and Src (Marinissen et al., 1999). Because Src and PKC are activated upstream of ERK1/2 in CHO-RXFP3, HEK-RXFP3, and SN56 cells after stimulation with H3 relaxin (van der Westhuizen et al., 2007), either pathway may be involved in increasing AP-1 transcription. Activation of NF-κB may occur via PI3K (Yuan and Yankner, 2000; Brunet et al., 2001), as seen for the δ-opioid receptor (Borlongan et al., 2004), or via PKC, as observed for the lysophosphatidic acid receptor (Shahrestanifar et al., 1999). ERK5 also activates NF-κB (Pearson et al., 2001), although direct activation was not studied here. PD98059 inhibited porcine relaxin-mediated activation of AP-1, suggesting that ERK5 may be activated by RXFP3. Because H3 relaxin activates ERK1/2 via PI3K and PKC (van der Westhuizen et al., 2007), either kinase may be important in RXFP3-mediated activation of NF-κB, although this remains to be empirically established.

H3 relaxin is the most potent activator of ERK1/2 and NF-κB and inhibitor of forskolin-stimulated cAMP accumulation in RXFP3-expressing cells. Signaling through these pathways is inhibited in cells pretreated with PTX, suggesting that $G\alpha_{i/o}$ is involved. Activation of these pathways probably occurs via the site or receptor conformations labeled with ^{125}I-INSL5/H3 relaxin, suggesting that H3 relaxin stabilizes RXFP3 conformations to enable coupling to NF-κB and ERK1/2 and inhibition of cAMP signaling. The profile observed for AP-1 activation resembled that of the ^{125}I-H2 relaxin binding site where H2 relaxin = H3 relaxin = INSL3 $\geq$ porcine relaxin. Porcine relaxin had poor affinity for this site, suggesting that it may bind to an alternative receptor conformation, possibly identifiable with ^{125}I-porcine relaxin, although this remains to be demonstrated. INSL3 also competed for H2 relaxin binding, suggesting that it interacts with RXFP3, although very few INSL3-preferring RXFP3 conformations are likely to be expressed because no ^{125}I-INSL3 binding was observed, and INSL3 had low potency for inhibition of forskolin-stimulated cAMP accumulation. Antagonism of RXFP3 by INSL3 was also examined, but INSL3 did not antagonize H3 or H2 relaxin-mediated ERK1/2 or AP-1 responses.

This study identifies novel signaling pathways activated by RXFP3. A second binding site identified on RXFP3 by ^{125}I-H2 relaxin seems to be coupled to signaling pathways linked to increased gene transcription from AP-1 sites, such as JNK, p38 MAPK, and ERK. These MAPKs are implicated in central stress and feeding responses, suggesting that their activation by H3 relaxin, H2 relaxin, and porcine relaxin may be important in RXFP3 function. The recognition that H2 relaxin and other related peptides can selectively activate particular signaling pathways may have significant implications for the design of drugs acting at RXFP3.

Acknowledgments

We thank Dr. Michelle L. Halls for assistance with developing the H2 relaxin iodination protocol and for assistance with the iodination of H2 relaxin and Brigham J. Hartley for completing some of the preliminary reporter gene assays. We also thank Dr. F. Lin and M. Akhter Hossain for synthesizing the H3 relaxin and chimeric INSL5/H3 relaxin peptides used in this study.

References

Alessi DR, Cuenda A, Cohen P, Dudley DT, and Saltiel AR (1995) PD 098059 is a specific inhibitor of the activation of mitogen-activated protein kinase kinase in vitro and in vivo. *J Biol Chem* **270:**27489–27494.

Bain J, Plater L, Elliott M, Shpiro N, Hastie CJ, McLauchlan H, Klevernic I, Arthur JS, Alessi DR, and Cohen P (2007) The selectivity of protein kinase inhibitors: a further update. *Biochem J* **408:**297–315.

Baker JG and Hill SJ (2007) Multiple GPCR conformations and signalling pathways: implications for antagonist affinity estimates. *Trends Pharmacol Sci* **28:**374–381.

Bathgate RA, Lin F, Hanson NF, Otvos L, Jr., Guidolin A, Giannakis C, Bastiras S, Layfield SL, Ferraro T, Ma S, Zhao C, Gundlach AL, Samuel CS, Tregear GW, and Wade JD (2006) Relaxin-3: improved synthesis strategy and demonstration of its high-affinity interaction with the relaxin receptor LGR7 both in vitro and in vivo. *Biochemistry* **45:**1043–1053.

Bathgate RA, Samuel CS, Burazin TC, Layfield S, Claasz AA, Reytomas IG, Dawson NF, Zhao C, Bond C, Summers RJ, et al. (2002) Human relaxin gene 3 (H3) and the equivalent mouse relaxin (M3) gene. Novel members of the relaxin peptide family. *J Biol Chem* **277:**1148–1157.

Borlongan CV, Wang Y, and Su TP (2004) Delta opioid peptide (D-Ala 2, D-Leu 5) enkephalin: linking hibernation and neuroprotection. *Front Biosci* **9:**3392–3398.

Brunet A, Datta SR, and Greenberg ME (2001) Transcription-dependent and -independent control of neuronal survival by the PI3K-Akt signaling pathway. *Curr Opin Neurobiol* **11:**297–305.

Chini B and Parenti M (2004) G-protein coupled receptors in lipid rafts and caveolae: how, when and why do they go there? *J Mol Endocrinol* **32:**325–338.

Davies SP, Reddy H, Caivano M, and Cohen P (2000) Specificity and mechanism of action of some commonly used protein kinase inhibitors. *Biochem J* **351:**95–105.

Davis RJ (2000) Signal transduction by the JNK group of MAP kinases. *Cell* **103:**239–252.

Galandrin S and Bouvier M (2006) Distinct signaling profiles of beta1 and beta2 adrenergic receptor ligands toward adenylyl cyclase and mitogen-activated protein kinase reveals the pluridimensionality of efficacy. *Mol Pharmacol* **70:**1575–1584.
Halls ML, Bathgate RA, and Summers RJ (2007) Comparison of signaling pathways activated by the relaxin family peptide receptors, RXFP1 and RXFP2, using reporter genes. *J Pharmacol Exp Ther* **320:**281–290.
Halls ML, Bond CP, Sudo S, Kumagai J, Ferraro T, Layfield S, Bathgate RA, and Summers RJ (2005) Multiple binding sites revealed by interaction of relaxin family peptides with native and chimeric relaxin family peptide receptors 1 and 2 (LGR7 and LGR8). *J Pharmacol Exp Ther* **313:**677–687.
Kamakura S, Moriguchi T, and Nishida E (1999) Activation of the protein kinase ERK5/BMK1 by receptor tyrosine kinases. Identification and characterization of a signaling pathway to the nucleus. *J Biol Chem* **274:**26563–26571.
Kenakin T (2003) Ligand-selective receptor conformations revisited: the promise and the problem. *Trends Pharmacol Sci* **24:**346–354.
Kuei C, Sutton S, Bonaventure P, Pudiak C, Shelton J, Zhu J, Nepomuceno D, Wu J, Chen J, Kamme F, et al. (2007) R3(BDelta23 27)R/I5 chimeric peptide, a selective antagonist for GPCR135 and GPCR142 over relaxin receptor LGR7: in vitro and in vivo characterization. *J Biol Chem* **282:**25425–25435.
Layden SS and Tregear GW (1996) Purification and characterization of porcine prorelaxin. *J Biochem Biophys Methods* **31:**69–80.
Liu C, Chen J, Kuei C, Sutton S, Nepomuceno D, Bonaventure P, and Lovenberg TW (2005) Relaxin-3/insulin-like peptide 5 chimeric peptide, a selective ligand for G protein-coupled receptor (GPCR)135 and GPCR142 over leucine-rich repeat-containing G protein-coupled receptor 7. *Mol Pharmacol* **67:**231–240.
Liu C, Eriste E, Sutton S, Chen J, Roland B, Kuei C, Farmer N, Jörnvall H, Sillard R, and Lovenberg TW (2003) Identification of relaxin-3/INSL7 as an endogenous ligand for the orphan G-protein-coupled receptor GPCR135. *J Biol Chem* **278:**50754–50764.
Marinissen MJ, Chiariello M, Pallante M, and Gutkind JS (1999) A network of mitogen-activated protein kinases links G protein-coupled receptors to the c-jun promoter: a role for c-Jun NH2-terminal kinase, p38s, and extracellular signal-regulated kinase 5. *Mol Cell Biol* **19:**4289–4301.
McGowan BM, Stanley SA, White NE, Spangeus A, Patterson M, Thompson EL, Smith KL, Donovan J, Gardiner JV, Ghatei MA, et al. (2007) Hypothalamic mapping of orexigenic action and Fos-like immunoreactivity following relaxin-3 administration in male Wistar rats. *Am J Physiol Endocrinol Metab* **292:**E913–919.
Osmond RI, Sheehan A, Borowicz R, Barnett E, Harvey G, Turner C, Brown A, Crouch MF, and Dyer AR (2005) GPCR screening via ERK 1/2: a novel platform for screening G protein-coupled receptors. *J Biomol Screen* **10:**730–737.
Pearson G, English JM, White MA, and Cobb MH (2001) ERK5 and ERK2 cooperate to regulate NF-kappaB and cell transformation. *J Biol Chem* **276:**7927–7931.
Price MA, Cruzalegui FH, and Treisman R (1996) The p38 and ERK MAP kinase pathways cooperate to activate ternary complex factors and c-fos transcription in response to UV light. *EMBO J* **15:**6552–6563.
Roux PP and Blenis J (2004) ERK and p38 MAPK-activated protein kinases: a family of protein kinases with diverse biological functions. *Microbiol Mol Biol Rev* **68:**320–344.
Sexton PM, McKenzie JS, Mason RT, Moseley JM, Martin TJ, and Mendelsohn FA (1986) Localization of binding sites for calcitonin gene-related peptide in rat brain by in vitro autoradiography. *Neuroscience* **19:**1235–1245.
Shahrestanifar M, Fan X, and Manning DR (1999) Lysophosphatidic acid activates NF-kappaB in fibroblasts. A requirement for multiple inputs. *J Biol Chem* **274:**3828–3833.
Shen CP, Tsimberg Y, Salvadore C, and Meller E (2004) Activation of Erk and JNK MAPK pathways by acute swim stress in rat brain regions. *BMC Neurosci* **5:**36.
Sutton SW, Bonaventure P, Kuei C, Roland B, Chen J, Nepomuceno D, Lovenberg TW, and Liu C (2004) Distribution of G-protein-coupled receptor (GPCR)135 binding sites and receptor mRNA in the rat brain suggests a role for relaxin-3 in neuroendocrine and sensory processing. *Neuroendocrinology* **80:**298–307.
Tanaka M, Iijima N, Miyamoto Y, Fukusumi S, Itoh Y, Ozawa H, and Ibata Y (2005) Neurons expressing relaxin 3/INSL 7 in the nucleus incertus respond to stress. *Eur J Neurosci* **21:**1659–1670.
van der Westhuizen ET, Wade JD, Sexton PM, and Summers RJ (2009) Addition of a carboxy-terminal green fluorescent protein does not alter the binding and signaling properties of relaxin family peptide receptor 3. *Ann NY Acad Sci* **1160:**105–107.
van der Westhuizen ET, Werry TD, Sexton PM, and Summers RJ (2007) The relaxin family peptide receptor 3 activates extracellular signal-regulated kinase 1/2 through a protein kinase C-dependent mechanism. *Mol Pharmacol* **71:**1618–1629.
Wadsworth SA, Cavender DE, Beers SA, Lalan P, Schafer PH, Malloy EA, Wu W, Fahmy B, Olini GC, Davis JE, et al. (1999) RWJ 67657, a potent, orally active inhibitor of p38 mitogen-activated protein kinase. *J Pharmacol Exp Ther* **291:**680–687.
Whitmarsh AJ and Davis RJ (1996) Transcription factor AP-1 regulation by mitogen-activated protein kinase signal transduction pathways. *J Mol Med* **74:**589–607.
Yuan J and Yankner BA (2000) Apoptosis in the nervous system. *Nature* **407:**802–809.

Address correspondence to: Prof. Roger J. Summers, Drug Discovery Biology, Monash Institute of Pharmaceutical Sciences, 399 Royal Parade, Parkville VIC 3052, Australia. E-mail: roger.summers@med.monash.edu.au